Passive Acoustic Thermometry Using Low-Frequency Deep Water Noise

Karim G. Sabra
School of Mechanical Engineering
Georgia Institute of Technology
Atlanta, GA 30332
Phone: (404) 385-6193 Fax(404) 894-1658 E-mail: karim.sabra@me.gatech.edu

Award number: N000141410228

LONG TERM GOALS

To develop a passive modality of acoustic thermometry using Cross-correlation processing of deep water ambient noise.

OBJECTIVE

Our previous research effort has demonstrated that coherent processing of shipping noise (100Hz<f<kHz) in shallow water can provide a totally passive means for sensing the ocean environment; but optimizing this correlation process for this relatively high frequency band remains challenging in a fluctuating ocean environment with significant multipath. We hypothesize that using instead significantly lower frequency (f<50Hz) ocean noise recorded in the SOFAR channel may enhance the performance of this correlation process due to the potential long-range spatial correlations (~100kms) of this deep water noise field and the relative temporal stability of the SOFAR channel.

The main objective of this year research was to assess the feasibility of passive (i.e. noise-based) acoustic thermometry using low-frequency deep water ambient noise recorded on the global IMS-CTBTO network Results from this study are expected to help guide the design of future cabled or autonomous ocean observatory systems for passive ocean monitoring**.**

WORK COMPLETED

Deep oceans play a major role in absorbing atmospheric heat, thus measuring deep oceans temperature variations is necessary among others to quantify air-sea heat exchanges- for instance to assess global warming trends (*1*) and calibrate climate change models (*2,3*). However, contrary to ocean surface temperatures, deep ocean temperatures cannot be readily inferred from satellite-based remote sensing methods (*4*) and are thus most commonly obtained in-situ using free-drifting profiling oceanographic floats but with limited spatial and temporal resolution as these floats only cover the globe sparsely *(5)*. Acoustic thermometry provides an alternative remote sensing modality for detecting fine variations in deep ocean temperatures based on acoustic propagation travel times between sources and receivers inserted in the ocean (*6*). Furthermore, a promising alternative to using active acoustic sources is based on noise correlation processing, which has successfully been used for continuously monitoring, with unprecedented temporal resolution, seismically-active systems such as fault zones (*6a*) and volcanic areas (*6b*). More generally, experimental and theoretical studies have demonstrated that an estimate of

the arrival time structure between two receivers for a given acoustic or elastic medium (as determined by the Green's function between the receivers locations) can be obtained from the time-averaged cross-correlation of the ambient noise recorded by the two receivers. This has been shown in the fields of ultrasonics (*9*,*10,10b*), helioseismology (*11,12*), seismology (*6,6a-6f*), structural health monitoring (*13a-13d*), and elastography (*14*). In the context of ocean acoustics, previous studies have demonstrated that the integration time required by this noise correlation method to reliably estimate the discrete acoustic paths traditionally used to infer temperature variations (*6*) is typically too long compared to the timescale of ocean fluctuations (*15-17*). However, for deep ocean propagation, there is an unusually stable acoustic feature- the last and most energetic arrival corresponding to sound propagating horizontally along the Sound Fixing and Ranging (SOFAR) channel- which can be estimated over a finite correlation time. The SOFAR channel is centered on the minimum value of the sound speed over the ocean depth and thus acts as a natural waveguide for long-range sound propagation (*18*). In this study, we demonstrate the feasibility of a totally passive (i.e. without using *any* controlled active sources) method for acoustic thermometry of the deep oceans using *only* records of low-frequency (f~10Hz) ambient noise propagating along the SOFAR channel. Estimates of deep ocean temperature variations obtained from this passive thermometry technique over several years are found to be consistent with oceanographic measurements obtained with classical free-drifting floats.

Here we used continuous recordings of ocean noise from two existing hydroacoustic stations of the International Monitoring System, operated by the Comprehensive Nuclear-Test-Ban Treaty Organization, located respectively next to Ascension and Wake islands (see Fig. 1A-B). Each hydroacoustic station is composed of two triangular-shaped horizontal arrays, separated by L~130km, which are referred to hereafter as the north and south triads (see Fig. 1C). The sides of each triad are ~2 km long and the three hydrophones are located within the SOFAR channel at depth ~1000m (*18b*). Examples of one-year-averaged noise cross-correlations in the frequency band [1Hz-40Hz] between pairwise combinations of hydrophones from the north and south triads appear in Fig. 1C-D. From year to year, the nearly identical coherent arrivals at time delays -corresponding to propagation between hydrophone pairs of the respective triads along the SOFAR channel axis- build up from noise sources whose paths intersect the sensor pairs. Based on the time-lag convention used for computing the correlation waveforms (*18b*), the coherent arrivals shown in Fig. 1C-D occurring at positive time delays are generated by coherent noise traveling northward, i.e. from the south triad to the north triad (see Fig. 1B). Conversely, negative time-delay arrivals correspond to coherent noise traveling southward in the opposite direction from the north triad to the south triad for the Wake Island site (*18b*). For the Ascension Island site, the African continent blocks most of the ocean noise propagating southward (see Fig. 1A) along the line connecting the north and south triads, so no coherent arrivals for negative time-lags could be extracted from the noise correlation waveforms at this site.

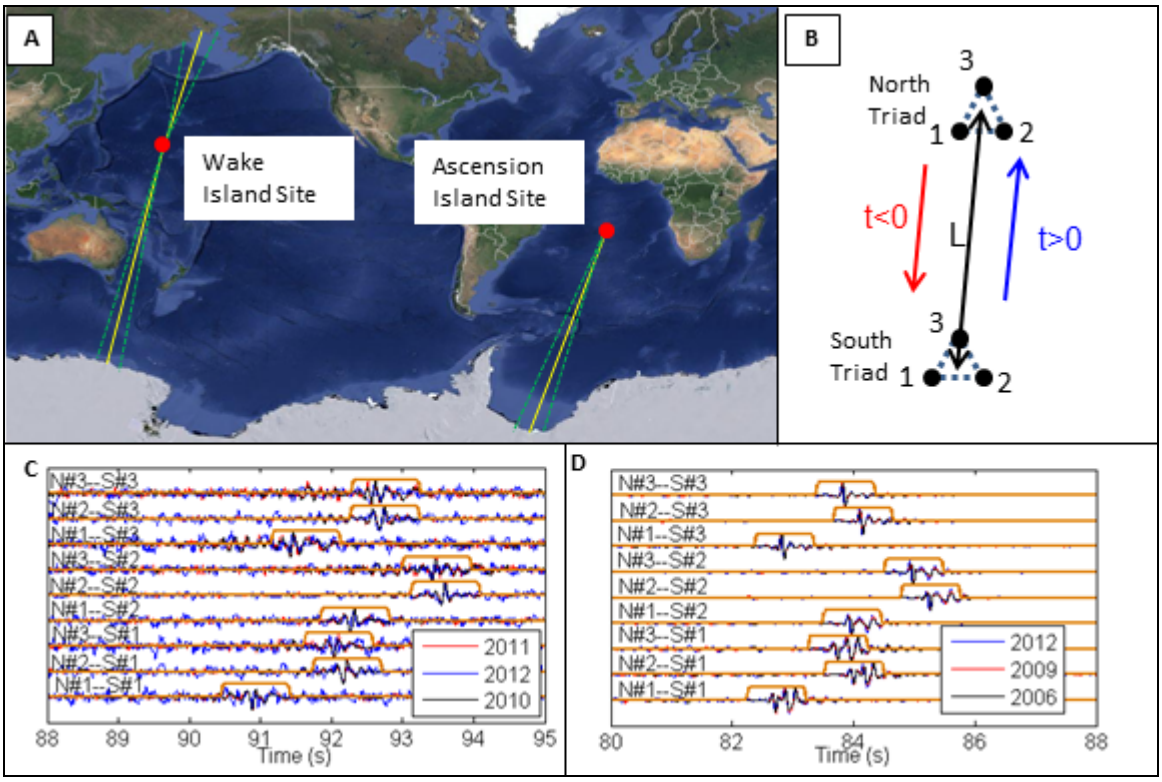

Fig. 1. (A) Locations of the two hydroacoustic stations (red dots) near Ascension and Wake Islands. Map data from Google Maps. (B) Zoomed-in schematic of the hydrophone array configurations for the Ascension and Wake Island sites, which both have a similar layout. Each hydroacoustic station consists of a northern and southern triangle array of three hydrophones (or triad), with each triangle side equal to approximately 2 km. The distance L between triad centers is equal to 126 km and 132 km for the Ascension and Wake Island stations, respectively. (C) Noise cross-correlation waveforms, averaged over three different years, obtained between all 9 pairwise combinations of the elements of the north and south triads for the Wake Island. (D) Same as C, but for Ascension Island. The beams shown by dashed lines in A are centered on the lines joining the centers of the south and north triads of each hydroacoustic station (yellow line) and which intersect the Polar regions where potential ice noise sources contributing to the coherent arrivals shown in C-D are located (18b).

In the low-frequency band used in this study (1-40Hz), where most of the acoustic energy is centered around 10 Hz, ambient noise propagating along the SOFAR channel mainly originates from seismic activity (e.g. along major undersea fault lines) or ice-breaking noise in the Polar Regions (*19-22*). Ice-generated ambient noise near the ocean surface in the Polar Regions (e.g. due to loud iceberg cracking events with levels up to 245 dB re 1 µPa at 1 m) can efficiently couple directly to the SOFAR channel due to the natural change in elevation of the minimum of the sound-speed profile from the sea surface in the cryosphere towards greater depths at lower latitudes where the Ascension and Wake Island sites are located (*21-23*). When using averaging durations shorter than 1 year, the observed seasonal variability of the amplitude of the coherent SOFAR arrivals- as show on Fig 1C-D- confirms the polar origin of the dominant component of the ambient noise generating these arrivals. The angular beams shown in Fig. 1A were extended all the way to the Arctic and Antarctic using geodesic paths to obtain a simple estimate of the geographical area from where ice-generated ambient noise is likely to emanate for each site. The bathymetry along the axis of this angular beam indicates that the Ascension Island site has a direct propagation line-of-sight with the Antarctica coastline, while at Wake Island

seamounts and islands partially block noise propagating from either the Arctic or Antarctica. This likely explains why the amplitudes of the arrivals exhibit a weaker peak-to-variance ratio for the Wake Island site when compared to the Ascension Island site (compare Fig 1C to 1D). An additional factor driving this difference in the peak-to-variance ratios is that the concentration of icebergs –which directly influences the ice noise source density and therefore the amount of coherent noise traveling along the SOFAR channel up to the hydroacoustic stations- is typically higher in the South Atlantic than in the South Pacific (*24*).

Acoustic thermometry estimates average oceanographic parameters, such as temperature variations, over large scales by leveraging the nearly linear dependency between sound speed in water and temperature (*25,6*) . Here a totally passive version of acoustic thermometry is used that monitors the fine temporal variations of the coherent SOFAR arrivals overall several years. These arrivals are obtained using a short averaging duration of 1 week, and are used to infer ocean sound speed variations within the SOFAR channel between the North and South triads at the Wake and Ascension Island sites. Here the SOFAR channel extends approximately from 390 m to 1350 m deep at the Ascension Island site and 460 m to 1600 m deep at the Wake Island site, as determined from the local sound speed profiles and the center frequency (~10Hz) of the SOFAR arrivals shown on Fig. 1C-D. This short one-week time-averaging was accomplished with a data analysis procedure based on using data averaged over 1 year, indicated by a time-gated box on Fig 1C-D, as a reference in a signal processing methodology (i.e., beamforming) that directionally combines the coherent arrivals collected between triads (*18b*). This process allows us to continuously track fine variations of the arrival- time structure with a one week temporal resolution over three years for Wake Island (Fig. 2A-B) and seven years for Ascension Island (Fig. 2C). These fine variations are indicative of mesoscale oceanic fluctuations occurring within the effective depth extent of the SOFAR channel over the range between triads. The 1 week-averaging duration was set conservatively to ensure a predicted error in arrival-time measurements (*18b*) of ~4 ms or less at the Wake Island site and ~1 ms or less at the Ascension Island site over the whole observation period. The observed fluctuations of the arrival-time errors across the years (indicated by the colorbars on Fig. 2), are primarily associated with Polar seasonal variations (*18b*).

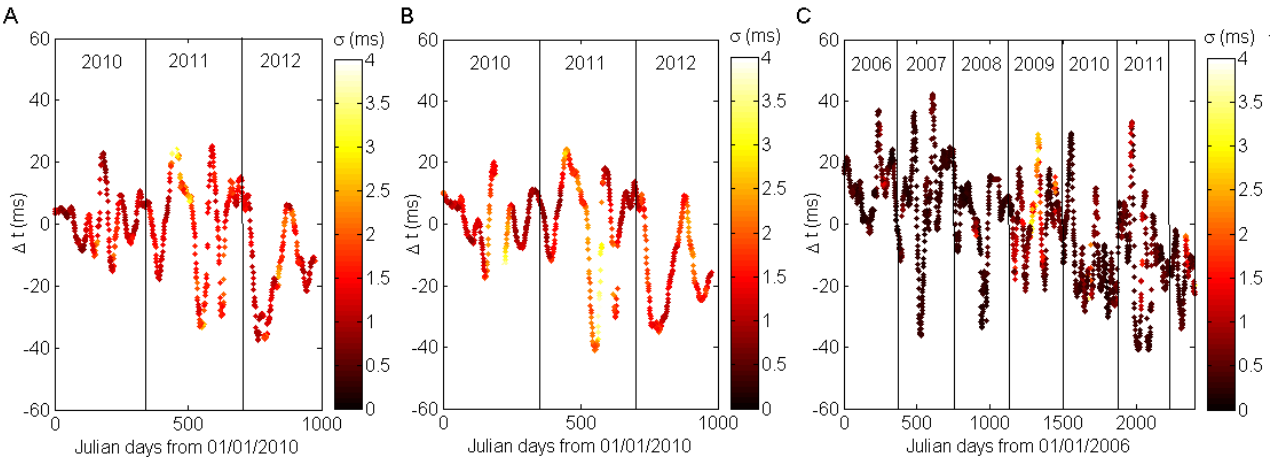

Fig. 2. (A) Temporal variations over 3 years of the coherent SOFAR arrivals at the Wake Island site extracted from ambient noise correlations using a one-week moving average. These arrivals primarily result from ice-noise originating propagating northward towards the Wake Island site successively from the South triad to the North triad. The color associated with each data point indicates the estimated measurement error σ in milliseconds (18b). (B) Same as A but using instead noise propagating southward towards the Wake Island site in the reciprocal direction i.e. successively from the North triad to the South triad. (C) Same as A but for noise propagating northward towards the Ascension Island site successively from the South triad to the North triad. Due to data availability a longer observation period of ~7 years was used for the Ascension Island site.

Comparing Fig. 2A and B demonstrates the similarity of the arrival-time variations obtained for both the positive and negative time-delay arrivals, which result from different noise events propagating northward or southward, respectively, along the same paths linking the south and north triads for the Wake Island site. This symmetry of the arrival-time variations (as confirmed in Fig. S2) demonstrates that they are due to reciprocal changes in the environment , such as ocean sound speed fluctuations induced by temperature changes, rather than non-reciprocal changes, such as currents, clock drift, or other signal-processing artifacts. (*26,27*). The symmetric arrival time variations could not be established for the Ascension Island site due to the African continent blockage of ocean noise propagating southward. Instead a spectral analysis of the arrival-time variations measured at Ascension Island from northward propagating noise, , confirmed a dominant period of 365 days, consistent with expected seasonal variations of the ocean sound speed at this site (*18b*).

Finally, the fine arrival-time variations with associated error bars were used to infer ocean temperature variations (*18b*) averaged over the effective depth extent of the SOFAR channel over several years between the North and South triads of the Wake Island and Ascension Island sites (see Fig. 3). In Fig. 3, overlaid dots correspond to estimated monthly temperature changes, and corresponding error bars, independently obtained from the Argo floats measurements (*5*) in the aforementioned effective depth of the SOFAR channel between the north and south triads of each hydroacoustic stations over the same time period. The magnitude of the temperature variations in the SOFAR channel estimated from passive thermometry and Argo data are in good agreement over the whole observation period, and the measurement error bars from passive thermometry are significantly smaller. An important methodology difference between these two estimates is that, given the sparseness of the global coverage by the Argo floats, the coarse Argo measurements are spatially and temporally interpolated to

provide monthly estimates of global temperature variations (*5*). On the other hand, passive thermometry measurements are not interpolated as they result from a true sampling of the ocean by propagating sound and thus integrates temperature variations over the whole propagation path (here ~130km between the North and South triads of each site) and averaging duration (here 1 week). Due to limited hydroacoustic data availability for the newly constructed Wake Island station, the observation period only covers 3 years, with one data point per month, and thus does not provide sufficient statistics for the Argo data to infer any significant long-term trend in ocean temperature variations. On the other hand, for the Ascension site, the SOFAR channel temperature variations measured over a longer duration of 7 years from passive thermometry and Argo are found to be significantly correlated with a 0.78 correlation coefficient, indicating that this passive thermometry method is sufficiently accurate to detect mesoscale variations of ocean temperatures occurring within the effective depth of the SOFAR channel. Furthermore, Fig. 3(B) indicates a warming of the SOFAR channel in the Ascension area as inferred from the similar upward trend of both passive thermometry (0.017 °C /year) and Argo (0.013 °C/ year) temperature variation estimates (*18b*); this finding is consistent with the recent report of increased heat transport to the deep southern Atlantic ocean over the same time period (1).

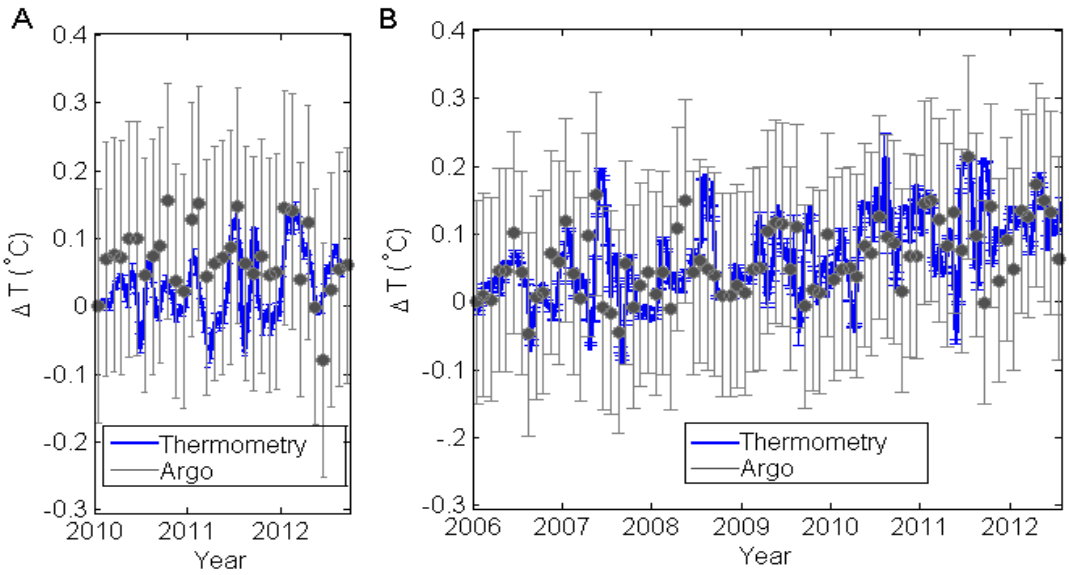

Fig. 3. (A) Comparison of the deep ocean temperature variations at the Wake Island site estimated from passive thermometry using the SOFAR arrival-time variations shown in Fig. 2A (blue line) with free-drifting profiling oceanographic Argo float measurements (grey dots), along with corresponding error bars (18b) (B) same as A, but for the Ascension Island site using the SOFAR arrival-time variations shown in Fig 2C.

Overall, the practical feasibility of passive thermometry is contingent upon extracting coherent arrivals with sufficient amplitude from noise correlations computed over the shortest possible averaging time T in order to accurately track temperature variations in a rapidly fluctuating ocean. Results from this study not only indicate that such signals can be obtained, but also that they can potentially be used to estimate the requirements of passive thermometry (in terms of achievable measurement error for a given averaging duration T) over longer receiver separation ranges, L, for temperature monitoring of deep oceans at basin scales. Indeed, previous studies have established that the $N{\cdot}M$ pairs of coherent arrivals extracted between the two hydrophone arrays each containing a different number of elements

N and *M*, respectively, can be jointly processed (via the beamforming procedure used in this study) to provide arrival-time variations from passive thermometry with an associated measurement error inversely proportional to $\sqrt{T/L}\sqrt{NM}$ (*17, 26, 28, 29*) ,where *L* is the separation distance between the centers of the two receiver arrays. Note that this simple scaling argument assumes that the statistics and generation mechanism of the Polar noise sources driving the longer range results remain comparable to the ones used in this study. Therefore, global monitoring of deep ocean temperature variations could be enabled with high sensitivity using this passive thermometry methodology by leveraging all pairwise combinations of a network of hydrophone arrays strategically deployed around the world.

CONCLUSIONS

The results of this research effort confirm the possibility of passive acoustic thermometry in the SOFAR channel. Further studies are required to fully assess the potential of noise-based ocean monitoring and tomography over very long observation periods and larger array separation distances.

IMPACT

It is conjectured that the results of this study could help develop a totally passive means for monitoring the ocean environment using only ambient noise. A potential scenario benefiting from the proposed methodology might include long-term deployment of ocean sensing systems requiring minimum power consumption, and for deployments where active sources are limited by environmental regulations.

PUBLICATIONS

Katherine F. Woolfe, Shane Lani, Karim G. Sabra, W.A. Kuperman, "Monitoring deep ocean temperatures using ambient noise" Manuscript in preparation (2014).

REFERENCES

1. X. Chen, K. Tung, Varying planetary heat sink led to global-warming slowdown and acceleration. *Science*. 345 , 897-903 (2014).
2. S. Häkkinen, P.B. Rhines, D. Worthen , Atmospheric Blocking and Atlantic Multidecadel Ocean Variability. *Science*. 334, 655-659, (2011).
3. T. Barnett, D. Pierce, K. Achuta-Rao, P. Gleckler, B.D. Santer, J.M. Gregory, W. Washington, W., Penetration of Human-Induced Warming into the World's Oceans. *Science*. 309, 284-287, (2005).
4. The ATOC Consortium, Ocean Climate Change: Comparison of Acoustic Tomography, Satellite Altimetry, and Modeling. *Science.* 281, 1327-1332, (1998).
5. D. Roemmich, J. Gilson, The 2004-2008 mean and annual cycle of temperature, salinity, and steric height in the global ocean from the Argo Program. *Prog. Oceanogr*. 82, 81-100, (2009).
6. W. Munk, P. Worcester, C. Wunsch, *Ocean Acoustic Tomography* (Cambridge University Press, Cambridge, 1995).

6a. F. Brenguier, M. Campillo, C. Hadziioannou, N.M. Shapiro, R.M. Nadeau, E. Larose, Postseismic

Relazation Along the San Andreas Fault at Parkfield from Continuous Seismological Observations. *Science*. 321, 1478-1481, (2008).

6b. F. Brenguier, M. Campillo, T. Takeda, Y. Aoki, N.M. Shapiro, X. Briand, K. Emoto, H. Miyake, Mapping Pressurized Volcanic Fluids from Induced Crustal Seismic Velocity Drops. *Science*. 345, 80-82, (2014).

6c. M. Campillo, A. Paul, Long-Range Correlations in the Diffuse Seismic Coda. *Science*. 299, 547-549, (2003).

6d. P. Poli, M. Campillo, H. Pedersen, and LAPNET Working Group, Body-Wave Imaging of Earth's Mantle Discontinuities from Ambient Seismic Noise. *Science*. 338, 1063-1065, (2012).

6e. N.M. Shapiro, M. Campillo, L. Stehly, M.H. Ritzwoller, High-Resolution Surface-Wave Tomography from Ambient Seismic Noise. *Science*. 307, 1615-1618, (2005).

6f. K.G. Sabra, P. Gerstoft, P. Roux, W.A. Kuperman, M.C. Fehler, Surface wave tomography from microseisms in Southern California. *Geophys. Res. Lett.* 32, L14311, (2005).

9. R.L. Weaver R.L., O. I. Lobkis, Ultrasonics without a source: Thermal fluctuation correlations at MHz frequencies.*Phys. Rev. Lett*. 87, 134301, (2001).

10. E. Larose, A. Derode, M. Campillo, M. Fink, M., Imaging from one-bit correlations of wideband diffuse wave fields. *J. Appl. Phys.* 95, 8393-8399, (2004).

10b. S. Lani, S. Satir, G. Gurun, K.G. Sabra, F.L. Degertekin, High-Frequency Ultrasonic Imaging Using Thermal Mechanical Noise Recorded on Capacitive Micromachined Transducer Arrays. *Appl. Phys. Lett.* 99, 224103, (2011).

11. T.L. Duvall, S.M. Jefferies, J.W. Harvey, M.A. Pomerantz, Time-distance helioseismology. *Nature*. 362, 430-432, (1993).

12. J. Rickett, J. Claerbout, Stanford Exploration Project Research Report No. SEP-92, (Stanford Univ., California, 1996) p.83. http://sepwww.stanford.edu/public/docs/sep92/james1/paper_html/index.html.

13a. K.G. Sabra, S. Huston, Passive structural health monitoring of a high-speed naval ship from ambient vibrations. *J. Acoust. Soc. Am*. 129, 2991-2999, (2011).

13b. R. Snieder, E. Cafak, Extracting the building response using seismic interferometry; theory and application to the Millikan Library in Pasadena, California. *Bull. Seismol. Soc. Am.* 96, 586-598, (2006).

13c. E. Larose, P. Roux, M. Campillo, Reconstruction of Rayleigh-Lamb dispersion spectrum based on noise obtained from an air-jet forcing. *J. Acoust. Soc. Am.* 122, 3437-3444, (2007).

13d. C. Farrar, G. James, System identification from ambient vibration measurements on a bridge. *J. Sound Vib.* 205, 1-18, (1997).

14. K.G. Sabra, A. Archer, Tomographic elastography of contracting skeletal muscles from their natural vibrations. *App. Phys. Lett.* 95, 203701 (2009).

15. P. Roux, W. Kuperman, the NPAL Group, Extracting coherent wave fronts from acoustic ambient noise in the ocean. *J. Acoust. Soc. Am*. 116, 1995-2003, (2004).

16. O. Godin, N. Zabotin, V. Goncharov, Ocean tomography with acoustic daylight. *Geophys. Res. Lett*. 37, L13605, (2010).

17. S. Fried, S.C. Walker, W.S. Hodgkiss, W.A. Kuperman, Measuring the effect of ambient noise directionality and split-beam processing on the convergence of the cross-correlation function. *J. Acoust. Soc. Am.* 134, 1824-1832, (2013).

18. M. Ewing, M., J.L. Worzel, Long-Range Sound Transmission. *GSA Memoirs.* 27, 1-32 , (1948).

18b. See supplementary materials on *Science* Online.

19. G.M. Wenz, Acoustic ambient noise in the ocean: Spectra and Sources. *J. Acoust. Soc. Am.* 34, 1936-1956, (1962).

20. A.R. Milne, J.H. Ganton, Ambient noise under Arctic-sea ice. *J. Acoust. Soc. Am.* 36, 855-864, (1964).

21. E. Chapp, D. Bohnenstiehl, M. Tolstoy, Sound-channel observations of ice-generated tremor in the Indian Ocean. *Geochem. Geophys. Geosyst.* 6, Q06003, (2005).

22. H. Matsumoto, D. Bohnenstiehl, J. Tournadre, R. Dziak, J. Haxel, T.K. Lau, M. Fowler, S. Salo, Antarctic icebergs: A significant natural ocean sound source in the Southern Hemisphere. *Geochem. Geophys.* DOI: 10.1002/2014GC005454, (2014).

23. J. Northrop, J.G. Colborn, Sofar channel axial sound speed and depth in the Atlantic Ocean. *J. Geophys. Res.* 79, 5633-5641, (1974).

24. J. Tournadre, F. Girard-Ardhuin, B. Legrésy, Antarctic icebergs distributions, 2002-2010. *J. Geophys. Res: Oceans* 117, C05004, (2012).

25. B. Dushaw, G. Bold, C.S. Chiu, J. Colosi, B. Cornuelle, Y. Desaubies, M. Dzieciuch, A. Forbes, F. Gaillard, A. Gavrilov, J. Gould, B. Howe, M. Lawrence, J. Lynch, D. Menemenlis, J. Mercer, P. Mikhalevsky, W. Munk, I. Nakano, F. Schott, U. Send, R. Spindel, T. Terre, P. Worcester, C. Wunsch, in *Observing the Oceans in the 21st Century*, (C. Koblinsky, N. Smith, Eds., Godae Project Office, Bureau of Meteorology, Melbourne, 2001), Ch. 4.4.

26. K.G. Sabra, P. Roux,W.A. Kuperman, Emergence rate of the time-domain Green's function from the ambient noise cross-correlation function. *J. Acoust. Soc. Am.,* 118, 3524-3531, (2005).

27. S. Lani, K.G. Sabra, W.S. Hodgkiss, W.A. Kuperman, P. Roux, Coherent processing of shipping noise for ocean monitoring. *J. Acoust. Soc. Am.* 133, EL108, (2013).

28. K.G. Sabra, P. Roux, A.M. Thode, G.L. D'Spain, W.S. Hodgkiss, W.A. Kuperman, Using Ocean Ambient Noise for Array Self-Localization and Self-Synchronization. *IEEE J. Ocean. Eng.*, 30, 338-347, (2005).

29. C. Leroy, S. Lani, K.G. Sabra, W.S. Hodgkiss, W.A. Kuperman, P. Roux, Enhancing the emergence rate of coherent wavefronts from ocean ambient noise correlations using spatio-temporal filters. *J. Acoust. Soc. Am.* 132, 883-893, (2012).

29b. F.B. Jensen, W.A. Kuperman, M.B. Porter, H. Schmidt, *Computational Ocean Acoustics, 2nd Edition*. Springer, New York, (2011).

29c. R.A. Locarnini, A. V. Mishonov, J. I. Antonov, T. P. Boyer, H. E. Garcia, O. K. Baranova, M. M. Zweng, and D. R. Johnson, *World Ocean Atlas 2009, Volume 1: Temperature.* S. Levitus, Ed. NOAA Atlas NESDIS 68, U.S. Government Printing Office, Washington, D.C., pp. 184 (2010).

29d. J.I. Antonov, D. Seidov, T. P. Boyer, R. A. Locarnini, A. V. Mishonov, H. E. Garcia, O. K. Baranova, M. M. Zweng, and D. R. Johnson, *World Ocean Atlas 2009, Volume 2: Salinity*. S. Levitus, Ed. NOAA Atlas NESDIS 69, U.S. Government Printing Office, Washington, D.C., pp. 184 (2010).

30. G.B. Kinda, Y. Simard, C. Gervaise, J.I. Mars, L. Fortier, Under-ice ambient noise in Eastern Beaufort Sea, Canadian Arctic, and its relation to environmental forcing. *J. Acoust. Soc. Am.* 134, 77-87, (2013).

31. K. Mackenzie, Nine-term equation for sound speed in the oceans. *J. Acoust. Soc. Am.*, 70, 807-812, (1981).